

## Provenance of present-day eolian dust collected off NW Africa

Jan-Berend Stuut, Matthias Zabel, Volker Ratmeyer, Peer Helmke,  
and Enno Schefuß

Research Center Ocean Margins, Universität Bremen, Bremen, Germany

Gaute Lavik

Max Planck Institute for Marine Microbiology, Bremen, Germany

Ralph Schneider

Département Géologie et Océanographie, UMR-CNRS 5805 EPOC, Université Bordeaux I, Talence, France

Received 25 June 2004; revised 22 October 2004; accepted 2 December 2004; published 23 February 2005.

[1] Atmospheric dust samples collected along a transect off the West African coast have been investigated for their physical (grain-size distribution), mineralogical, and chemical (major elements) composition. On the basis of these data the samples were grouped into sets of samples that most likely originated from the same source area. In addition, shipboard-collected atmospheric meteorological data, modeled 4-day back trajectories for each sampling day and location, and Total Ozone Mapping Spectrometer aerosol index data for the time period of dust collection (February–March 1998) were combined and used to reconstruct the sources of the groups of dust samples. On the basis of these data we were able to determine the provenance of the various dust samples. It appears that the bulk of the wind-blown sediments that are deposited in the proximal equatorial Atlantic Ocean are transported in the lower level ( $\geq 900$  hPa) NE trade wind layer, which is a very dominant feature north of the Intertropical Convergence Zone (ITCZ). However, south of the surface expression of the ITCZ, down to  $5^{\circ}\text{S}$ , where surface winds are southwesterly, we still collected sediments that originated from the north and east, carried there by the NE trade wind layer, as well as by easterly winds from higher altitudes. The fact that the size of the wind-blown dust depends not only on the wind strength of the transporting agent but also on the distance to the source hampers a direct comparison of the dust's size distributions and measured wind strengths. However, a comparison between eolian dust and terrigenous sediments collected in three submarine sediment traps off the west coast of NW Africa shows that knowledge of the composition of eolian dust is a prerequisite for the interpretation of paleorecords obtained from sediment cores in the equatorial Atlantic.

**Citation:** Stuut, J.-B., M. Zabel, V. Ratmeyer, P. Helmke, E. Schefuß, G. Lavik, and R. Schneider (2005), Provenance of present-day eolian dust collected off NW Africa, *J. Geophys. Res.*, 110, D04202, doi:10.1029/2004JD005161.

### 1. Introduction

[2] The first written observations of eolian dust over the open ocean probably stem from the second half of the twelfth century, when the explorer Edrisi (1100–1166) found dust on his ship during his expeditions off northwestern Africa. More than 6 centuries later, Matthew Dobson published one of the first papers on the Harmattan wind system [Dobson, 1781], followed in 1846 by Charles Darwin, who observed eolian dust off the northwestern African coast during one of his expeditions with the “Beagle” [Darwin, 1846]. Since then, numerous papers have appeared on studies concerning eolian dust [e.g., Carlson and Prospero, 1972; Chester and Johnson, 1971;

Pye, 1987; Rea, 1994, and references therein]. Recently, the great sensitivity of dust emissions to climate has been recognized, not only for the potential feedback mechanism of dust production and desertification [Prospero and Lamb, 2003] but also for the various roles eolian material deposited to the ocean surface may potentially have; in some cases it may be responsible for new production in areas where the iron-rich dust acts a fertilizer [Martin and Fitzwater, 1988], whereas in other regions it may cause starvation of marine organisms, e.g., because of the fungi carried along with the dust [Shinn *et al.*, 2000].

[3] Most attention obviously was paid to the Saharan desert as a source of eolian dust, since it is the largest desert in the world with estimated modern dust production rates ranging from 130 to  $700 \times 10^6$  t/yr [d'Almeida, 1989; Schütz *et al.*, 1981; Swap *et al.*, 1996], about one third of which is deposited in the North Atlantic Ocean [Duce *et al.*,

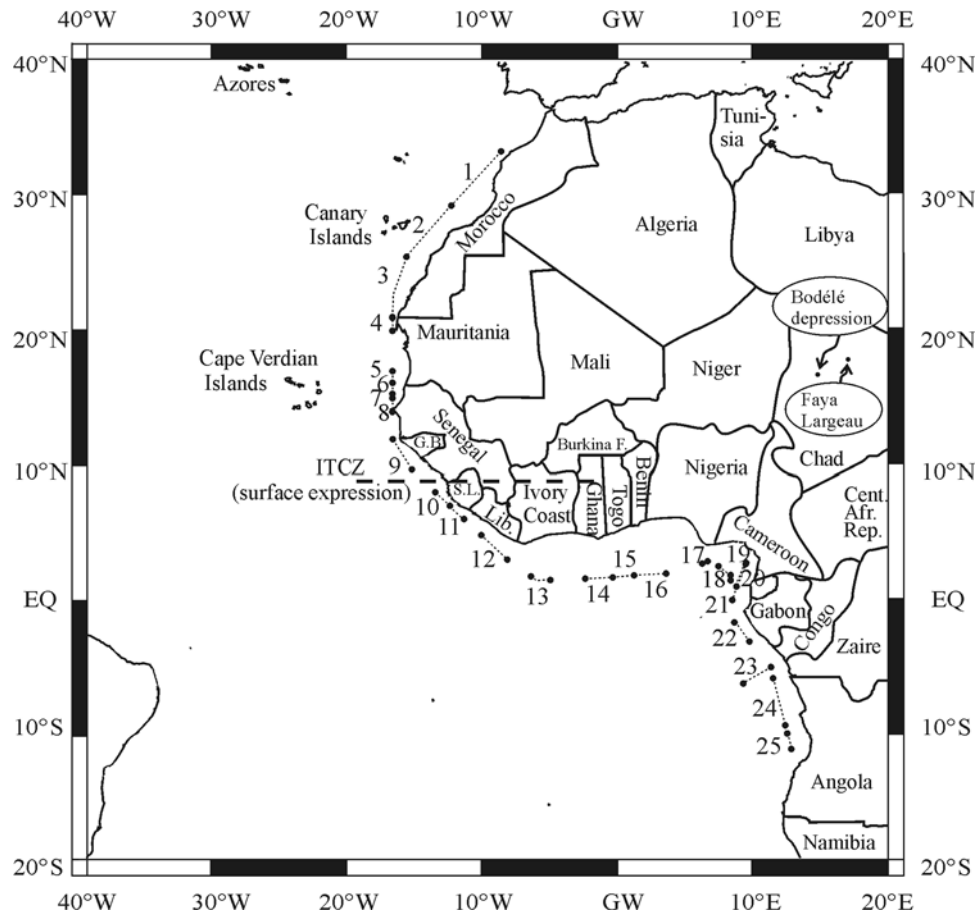


**Figure 1.** Ship track and dust sampling sites of R/V *Meteor* cruise M41/1 along the West African margin. Dust samples were taken between the points indicated.

1991]. The large spread in these estimates most likely has to be explained by the different methods used. However, the Sahel region, one of the source areas of northwest African dust, has suffered from varying degrees of drought since 1970 [e.g., Prospero and Lamb, 2003]. Therefore the aforementioned amounts may well be underestimations.

[4] Since the last few decades the enormous spread of (Saharan) dust outbreaks can be witnessed using satellite imagery; hence the identification of the Faya Largeau, Chad, as the key source area of NW African eolian dust [McTainsh and Walker, 1982] was confirmed using satellite images [e.g., Prospero et al., 2002], but also present-day dust pathways can be witnessed. Thus dust plumes originating from the Sahara have been observed to reach as far west as the Bahamas [e.g., Ott et al., 1991]. Indeed, eolian dust deposits have been found on the Canary Islands [e.g., Rognon and Coudé-Gaussen, 1996] and Cape Verde Islands [e.g., Glaccum and Prospero, 1980], in South America [Prospero et al., 1981], and in Florida and Barbados [Glaccum and Prospero, 1980; Muhs et al., 1990]. Several selective transport mechanisms were recognized along the pathways of dust: downwind decrease in grain size of the wind-blown material from  $\sim 90 \mu\text{m}$  on the Cape Verde Islands [Glaccum and Prospero, 1980] to  $\sim 5 \mu\text{m}$  in the Caribbean [Talbot et al., 1986] and downwind depletion of quartz grains and enrichment of clay minerals, related to the relatively larger mass median diameter of quartz, and,

consequently, its greater settling velocity in the atmosphere [Glaccum and Prospero, 1980].

[5] Eolian dust found in equatorial North Atlantic deep marine sediments has been used to reconstruct paleoenvironmental changes in northwestern Africa. Since the majority of land-derived sediments in this part of the Atlantic Ocean are of eolian origin, often the terrigenous sediment fraction was taken to be wind blown [deMenocal et al., 2000; Moreno et al., 2001; Sarnthein et al., 1982], although admixture of fluvial-transported or laterally advected sediments was found to play a role as well [Holz et al., 2004; Koopmann, 1981; Rattmeyer et al., 1999; Zabel et al., 1999].

[6] In summary, eolian dust is widely recognized as a potential major player and recorder of environmental change, but there appear to be large gaps in our knowledge about the location of source areas; source-to-sink selective transport processes; the actual properties of the aerosols in terms of particle size, chemistry, and mineralogy; as well as the influence of atmospheric transport processes on the amount as well as the composition of the transported dust. This is partly due to the fact that most information available about wind-blown dust is not obtained from the actual aerosols but is instead derived from marine sediments that apparently contain a large portion of eolian dust.

[7] Here we present physical (grain-size distributions), mineralogical, and chemical (major elements) data of 25 aerosol samples, collected along a transect from

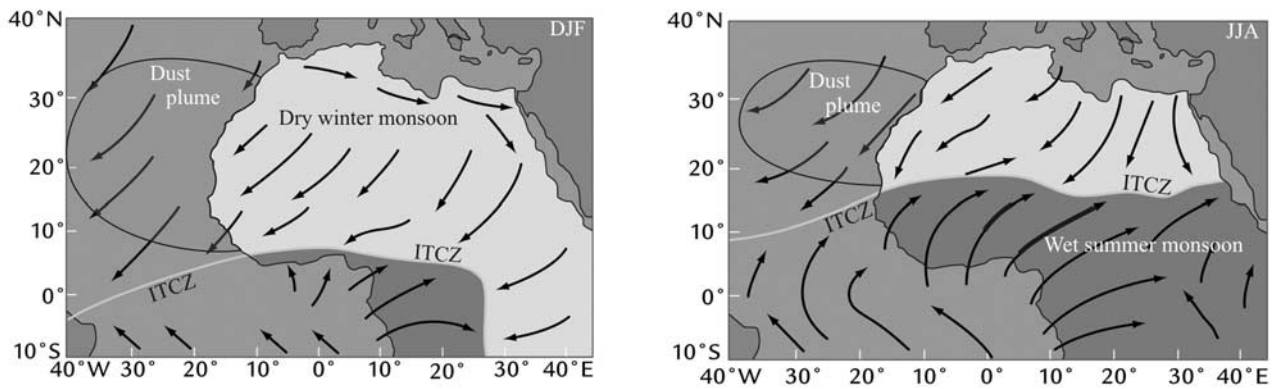


**Figure 2.** Seasonal variation in latitudinal position of the ITCZ and its consequences for atmospheric conditions over northwestern Africa (modified after Ruddiman [2001]). Arrows indicate direction of trade winds; dust plumes are indicated by grey shadings. December, January, and February (DJF) and June, July, and August (JJA) are shown.

$\sim 33^{\circ}\text{N}/10^{\circ}\text{W}$  to  $\sim 12^{\circ}\text{S}/13^{\circ}\text{E}$  (D1 to D25) along the northwestern African coast in February and March 1998 (Figure 1). These samples were taken during one of the largest Saharan dust outbreaks of the late twentieth century over the Canary archipelago [Pérez-Marrero *et al.*, 2002]. In combination with the local and regional meteorological data, obtained on the locations of the sample sites [Schulz *et al.*, 1998], as well as Total Ozone Mapping Spectrometer (TOMS) data, the observed variations in grain size and chemical composition are discussed relative to the provenance of the dust from potential source areas on the adjacent continent. Four-day back trajectory data of the level of highest transport capacities for each individual sample were calculated to further locate the source of each individual dust sample. These data provide insight into the sources and transport pathways of terrigenous sediments that are blown into the ocean from the northwestern African continent.

## 2. Regional Setting

[8] The most important atmospheric feature over northwestern Africa is the seasonal latitudinal shift of the Intertropical Convergence Zone (ITCZ) from  $\sim 19^{\circ}\text{N}$  during boreal summer to  $\sim 5^{\circ}\text{S}$  during winter [e.g., Hamilton and Archbold, 1945] (see Nicholson [2000] and Figure 2). The ITCZ separates the northern and southern Hadley cells and forms the location where the northeastern and southeastern trade winds meet. However, the vertical structure of the ITCZ is not a perpendicular one but tilted toward the north during both summer and winter [Hastenrath, 1985]. During boreal summer the angle is less steep compared to the boreal winter situation, potentially leading to more dust deposition south of the surface position of the ITCZ. The seasonal shift of the ITCZ obviously has large effects on both the origin of the eolian dust and the pathways of the transported dust [Husar *et al.*, 1997; Middleton and Goudie, 2001].

[9] A specific part of the northeast trades originates from the alluvial plain of Bilma (Niger) and Faya Largeau (Chad, Figure 1), and is called the Harmattan [e.g., Hamilton and Archbold, 1945; Kalu, 1979; McTainsh, 1980]. The Harmattan (Tuareg for “wind that carries dust”) is one of the

best studied wind systems in the world [e.g., Dobson, 1781; Koopmann, 1981; McTainsh, 1980; McTainsh and Walker, 1982; Simoneit *et al.*, 1988; Wilke *et al.*, 1984]. This cold and dry wind system is particularly known to carry large amounts of nutrient-rich eolian dust, picked up from the nearby Bodélé depression [e.g., Prospero and Lamb, 2003], which makes this wind system a fertilizer for Nigerian soils [Wilke *et al.*, 1984]. The winds blow from  $\sim 30^{\circ}$  north latitude to coastal West Africa, sometimes reaching as far south as the equator [Oliver and Fairbridge, 1987]. On reaching the ITCZ over southern Nigeria, the dust-laden Harmattan air is undercut by warm and moist tropical air and raised to a higher level (750–600 hPa) over the equatorial Atlantic [Pye, 1987].

[10] The upper level flow in the atmosphere during boreal winter is westerly, due to the equatorward displacement of the northern westerlies [e.g., Nicholson, 2000]. These westerlies are also denominated “anti trades” [Hamilton and Archbold, 1945].

[11] During boreal summer, when the ITCZ moves northward over the African continent, surface airflow over the northwestern African continent is dominated by the humid SW monsoon flow south of the ITCZ and the NE trades north of the ITCZ (see Nicholson [2000] and Figure 2). However, upper air patterns are completely reversed and change to easterly during these months [e.g., Prospero, 1996]. The easterlies consist of three jet streams; a small easterly jet at  $\sim 10^{\circ}\text{S}$ , the Tropical Easterly Jet, and the African Easterly Jet (AEJ). The AEJ, also called the Saharan Air Layer (SAL) [e.g., Pye, 1987], is the most important of the three, since it provides energy for the development and maintenance of rain-bearing disturbances [Nicholson, 2000] and carries dust at a height of  $\sim 3$  km [Pye, 1987]. This easterly flow is characterized by a series of large waves that propagate westward at an average velocity of 8 m/s, crossing the coast between latitudes  $15^{\circ}$  and  $21^{\circ}\text{N}$  [Reed *et al.*, 1977]. The outbreaks of dust-laden Saharan air travel above the surface trade wind layer and generally take 5–6 days to cross the Atlantic Ocean [Carlson and Prospero, 1972; Prospero, 1990; Pye, 1987]. Quite frequently, however, the flow at the 700-hPa level develops a strong

**Table 1.** Positions and Total Sampling Time of All Dust Samples ( $N = 25$ ) and Maximum Wind Speed, Wind Direction, Altitude, and Pressure, Respectively, of the Layer of Maximum Transporting Capacity, Determined from the Atmospheric Profiles as Measured by Weather Balloons From the Deutsche Wetterdienst Onboard FS *Meteor* During Cruise M41/1, February–March 1998

Sample	Start	End	Sampling Time, hours	Top Wind Speed, cm/s	Wind Direction, deg.	Altitude, m asl <sup>a</sup>	Pressure, hPa
1	32°24'64"N/9°54'32"W	28°29'28"N/13°26'54"W	11.8	1690	156	457	975
2	28°25'15"N/13°30'45"W	24°55'75"N/16°53'12"W	10.6	1072	122	391	980
3	24°55'75"N/16°53'12"W	20°16'47"N/17°55'08"W	8.3	1341	94	305	985
4	20°11'72"N/17°54'91"W	19°16'4"N/17°54'8"W	4.4	1341	94	305	985
5	16°22'72"N/17°54'95"W	15°37'01"N/17°54'93"W	5.0	1058	90	310	980
6	15°37'01"N/17°54'93"W	14°57'11"N/17°55'16"W	2.8	1058	90	310	980
7	14°57'11"N/17°55'16"W	14°26'28"N/17°55'08"W	2.0	no data	no data	no data	no data
8	14°26'28"N/17°55'08"W	13°24'41"N/17°54'88"W	4.4	no data	no data	no data	no data
9	11°26'18"N/17°52'40"W	09°05'77"N/16°14'01"W	7.6	1070	1	474	960
10	07°44'01"N/14°42'64"W	06°47'15"N/13°38'69"W	7.0	1360	76	2152	790
11	06°45'41"N/13°36'79"W	05°49'06"N/12°34'01"W	7.0	no data	no data	no data	no data
12	04°31'61"N/11°07'83"W	02°53'38"N/09°18'72"W	13.1	1686	83	2595	750
13	01°30'57"N/07°46'81"W	01°04'74"N/06°06'00"W	9.5	1710	57	2708	740
14	01°14'27"N/03°51'40"W	01°23'23"N/01°51'20"W	10.9	1770	64	1939	810
15	01°23'23"N/01°51'20"W	01°38'90"N/00°39'12"E	12.8	1770	64	1939	810
16	01°38'90"N/00°39'12"E	01°51'14"N/02°36'84"E	9.9	959	32	2041	800
17	02°39'27"N/06°40'17"E	02°24'00"N/06°03'00"E	8.8	1471	75	3176	700
18	02°04'87"N/07°21'72"E	01°01'80"N/08°10'00"E	7.7	1080	80	3418	680
19	00°58'41"N/08°53'16"E	02°30'00"N/09°23'01"E	8.8	no data	no data	no data	no data
20	02°19'94"N/09°20'09"E	00°56'71"N/08°52'82"E	7.8	no data	no data	no data	no data
21	00°41'31"S/08°22'64"E	02°03'87"S/08°38'72"E	8.1	940	85	3351	685
22	02°04'73"S/08°37'87"E	03°43'82"S/09°47'09"E	10.6	780	52	2523	755
23	05°30'50"S/11°03'61"E	06°50'41"S/09°02'24"E	13.7	539	42	3044	710
24	06°12'50"S/11°18'95"E	10°14'35"S/12°22'25"E	21.8	296	198	411	965
25	11°28'09"S/12°50'92"E	09°55'00"S/12°08'00"E	9.8	no data	no data	no data	no data

<sup>a</sup>Above sea level.

southerly component in the lee of an easterly wave, and after crossing the African coast, the dust outbreak moves first northwest and then northward, forming a hook-like trajectory between the Cape Verde Islands and the Canary Islands [Pyre, 1987], often recognized on satellite images.

[12] In summary, generally three wind systems are responsible for transporting dust across northwestern Africa [Pyre, 1987; Wilson, 1971]. First, in the northwest Sahara, dust is transported all year round in the shallow trade wind layer from the Atlas Mountains and coastal plain in a direction almost parallel to the coast. This wind system carries dust to the proximal parts of the Atlantic Ocean; a zone extending from the coast to the Canary Islands and Cape Verde Islands [Pyre, 1987, and references therein]. Second, dust from the central Sahara is carried by the Harmattan wind system, a particular expression of the northeast trades. This wind system is also a year-round feature, however, with highest intensities during boreal winter. Third, the SAL carries dust at midtropospheric levels, predominantly during boreal summer. By far, the largest amount of dust is transported to the ocean by the NE trades [Swap *et al.*, 1996]; this is partially caused by the fact that the mass flux of dust via dry deposition can be controlled by a relatively small fraction of aerodynamically large particles [Arimoto *et al.*, 1997]. The dust that is carried by the SAL, however, has a fairly large influence on global climate affecting the radiative balance and chemical composition of the atmosphere [Kohfeld and Harrison, 2001]. Still, due to the relatively fine grain sizes and widespread distribution of this “long-distance dust,” its contribution to marine sediments is relatively small compared to the “prox-

imal dust” brought to the equatorial Atlantic by the trade winds.

### 3. Material and Methods

[13] Dust samples ( $N = 25$ ) were collected along a transect from  $\sim 33^\circ\text{N}$  to  $12^\circ\text{S}$ , along the northwestern African coast (Figure 1) using two parallel dust samplers consisting of a metal-roofed house with a vacuum-cleaner engine sucking  $1.2\text{--}2.0\text{ m}^3$  air per min through about letter-size ( $200 \times 250\text{ mm}$ ) filters, which were located at  $\sim 10\text{ m}$  above sea level (asl). The filters were exposed between 17 February 1998 and 9 March 1998. Exposure times depended on the amount of dust and varied from  $\sim 2$  to more than 20 hours [see Schulz *et al.*, 1998]. Two types of filters were used, one in each dust sampler: cellulose filters for inorganic samples on which the grain-size analyses and bulk chemical analyses were performed and glass-fiber filters for organic analyses (C and N isotopes from G. Lavik *et al.* (unpublished results, 2000) and C isotopes of high-plant biomarkers from Schefuß *et al.* [2003]). For the grain-size analyses the dust was rinsed off the filters following the method described by Kiefert [1994] and Kiefert *et al.* [1996] using demineralized water instead of trisodium orthophosphate [Stuut, 2001]. This way, all samples were “minimally dispersed” in order to prevent the breaking up of aggregates. The filters appeared to have a size-independent efficiency of  $\sim 60\%$  [Stuut, 2001]. Particle sizes were measured with the Coulter laser particle sizer (LS230) at the Royal Netherlands Institute for Sea Research, Texel, Netherlands, resulting in minimally dispersed particle-size distributions from  $0.04\text{--}2000\text{ }\mu\text{m}$ . The material of two

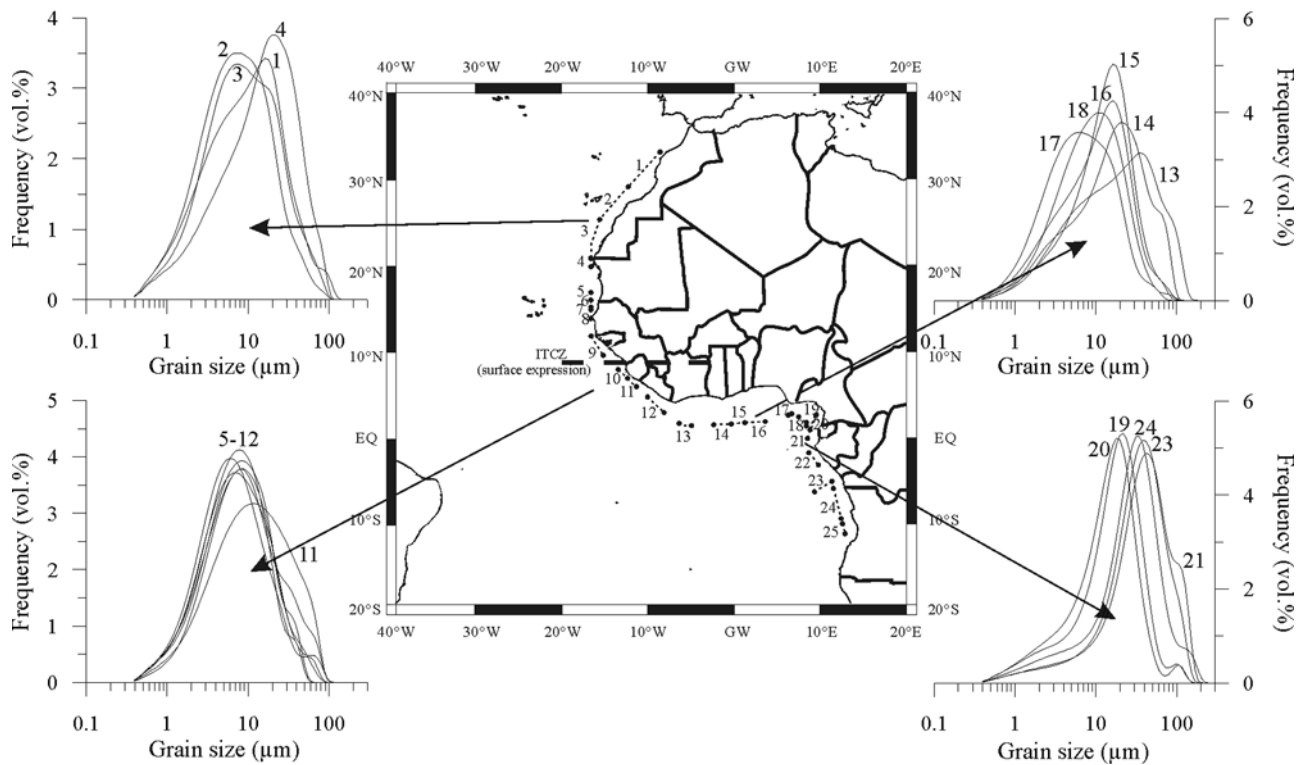


**Figure 3.** Grouped grain-size distributions of all samples. Four groups were distinguished: (top left) samples 1–4, (bottom left) samples 5–7 and 9–12, (top right) samples 13–18, and (bottom right) samples 19–21 and 23–24.

samples (8 and 22) was contaminated during analysis and was therefore not considered in this study.

[14] Element analysis was carried out at the Fachbereich Geowissenschaften of the Bremen University using an inductively coupled plasma atomic emission spectrometer (Perkin Elmer, Optima 3300RL), following the procedure described by *Zabel et al.* [2001]. The material of four samples could not be analyzed because the samples either were contaminated (8 and 22) or contained too few material to be analyzed (21 and 25). Therefore these samples were not considered in this study.

[15] All samples were analyzed by X-ray diffraction to determine their mineral composition, applying Cu K $\alpha$  radiation ( $\lambda = 1.5418 \text{ \AA}$ ). Before analysis the bulk samples were Ca exchanged and after that dried at 60°C. Non-oriented specimens were prepared pressing an amount of this material in a depression in a metal plate. For details on instrumentation and methodology, see *Van der Gaast* [1991]. Individual peaks of characteristic minerals (smectite, illite, kaolinite, quartz, and mica) were identified and quantified relatively using a normalization of the respective peak heights of the individual minerals to the total amount of counts.

[16] Four-day back trajectories were calculated using the Hybrid Single-Particle Lagrangian Integrated Trajectory (HY-SPLIT 4) model of National Oceanic and Atmospheric Administration (NOAA) (HY-SPLIT model access available from NOAA Air Resources Laboratory Real-time Environmental Applications and Display System (READY) at <http://www.arl.noaa.gov/ready/hysplit4.html>) to calculate daily 4-day backward trajectories at the levels that appeared

from the daily meteorological data to most likely carry the largest dust loads (see Table 1, level of trajectory per individual sample, for which atmospheric profiles were available).

[17] Daily TOMS (<http://jwocky.gsfc.nasa.gov>) data were used to identify outbreaks of dust from 10 February (a week before the dust sampling started) until 9 March 1998. For details of the TOMS aerosol index method see *Chiapello et al.* [1999] and *Herman et al.* [1997].

## 4. Results

### 4.1. Grain Size

[18] The grain-size distributions of the dust samples nearly all show well-sorted unimodal distributions (Figure 3), which is a well-known characteristic of wind-blown sediments [e.g., *Krumbein and Pettijohn*, 1938]. Generally, mean modal sizes range from about 8–42  $\mu\text{m}$ , but frequently particles of up to 200  $\mu\text{m}$  do occur. A number of samples show a small peak at the coarse side of the main peak (e.g., samples 19 and 20 but also 9 and 10) that is caused by platy particles which have “equal-area sizes,” as measured by the laser particle sizer, that are larger than their respective “hydrodynamic sizes,” as would have been measured by a settling technique [see, e.g., *Konert and Vandenberghe*, 1997]. There is, however, a large spread in the actual size distributions, on the basis of which different regions can be classified. Samples 1–4 (off Morocco, Western Sahara, and northern Mauritania) show no clear trend in size-distribution shape, nor modal values, whereas samples 5–12 (off Mauritania and Senegal, down to Liberia) show comparable

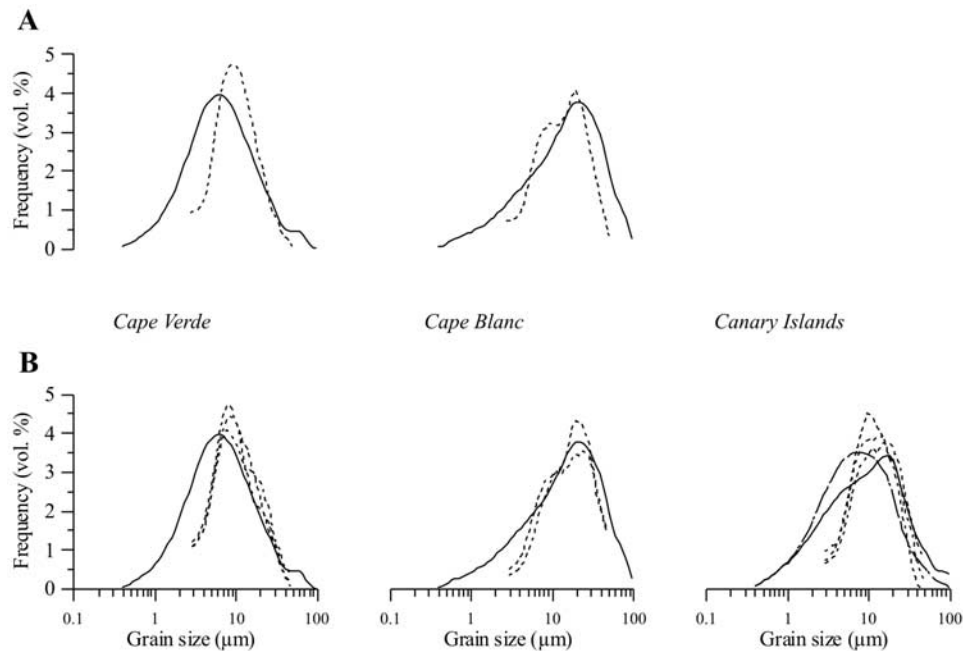


**Figure 4.** Comparison of grain-size distributions of aerosol samples with sediment trap and surface sediment samples collected at approximately the same locations [Ratmeyer *et al.*, 1999]. (a) Sediment trap samples at 200-m water depth compared with aerosol samples. At Cape Verde, CV10-17 (dashed line) and sample D9 (solid line) are shown, and at Cape Blanc, CB1-5 (dashed line) and sample D4 (solid line) are shown. (b) Surface sediment samples compared with present-day dust samples. At Cape Verde, three samples from multicore GeoB 2911, 5020-m water depth (dashed lines), and D9 (solid line) are shown. At Cape Blanc, two samples from core GeoB 2912, 4136-m water depth (dashed lines), and D4 (solid line) are shown. At Canary Islands, three samples from core GeoB 2913, 3621-m water depth (short-dashed lines), and D1 and D2 (solid and long-dashed lines, respectively) are shown.

sizes (mean modal size around 9  $\mu\text{m}$ ) as well as shapes of the size distributions, with the exception of sample 11, which is coarser grained (mean modal size around 18  $\mu\text{m}$ ). Samples 13–18 (off Ivory Coast to Cameroon) show a gradual fining in the size distributions from  $\sim 40$   $\mu\text{m}$  (sample 13) down to  $\sim 10$   $\mu\text{m}$  (sample 17). Samples 19–24 (off Cameroon down to Congo) all show negatively skewed distributions with modal values ranging from about 18–42  $\mu\text{m}$ .

[19] The observed grain-size distributions compare relatively well to grain-size distributions from the terrigenous sediment fraction collected in sediment traps (Figure 4a) and surface sediments below the traps (Figure 4b [from Ratmeyer *et al.*, 1999]). Especially the grain-size distributions of aerosols, trap, and sediment surface samples from off Cape Blanc resemble each other very well (Figures 4a and 4b). The trap sample from off Cape Verde (Figure 4a) is slightly finer grained than the aerosol sample, whereas the surface sediment distribution is slightly coarser grained (Figure 4b). No trap samples were available for the Canary Islands site, but the sediment surface sample (Figure 4b) is again coarser grained than the aerosol sample.

#### 4.2. Bulk Chemistry

[20] The bulk chemistry analyses of the dust samples partly confirm the interpretation of the grain-size distributions regarding their grouping. The most obvious trends can

be seen in the elements Ti, Fe, and Al (Figures 5a–5c); samples 1–4 show no clear trend, whereas samples 5–10 reveal a more or less constant chemical composition. On the basis of bulk chemistry, however, samples 11–13 show a decreasing trend in all elements, and samples 14–20 show a more or less constant chemical composition. Unfortunately, no results could be obtained for samples 21 and 22 because of contamination and low amounts of material. Samples 23 and 24 show a deviating chemical composition again, possibly indicating yet another source area. The variability in the Ti/Al ratio throughout the samples falls (with the exception of sample 1) exactly within the range that was observed in deep sea sediments in the central equatorial Atlantic Ocean (Ti/Al = 0.04–0.08 [Zabel *et al.*, 1999]) and in the eastern equatorial Atlantic Ocean (Ti/Al = 0.04–0.07 [Zabel *et al.*, 2001]; Figure 5d).

#### 4.3. Bulk Mineralogy

[21] The bulk mineralogical composition (Figures 5d–5i) supports the grouping of samples on the basis of their grain-size distributions. Especially the amounts of kaolinite indicate that samples 5–9, but most probably also 10 and 11, originate from about the same source. The illite/kaolinite ratio, a proxy that was shown to remain unchanged even after long-range transport [Caquineau *et al.*, 1998], does not reveal any clear trend throughout the data set, except for a slight general decrease from north to south. A comparison

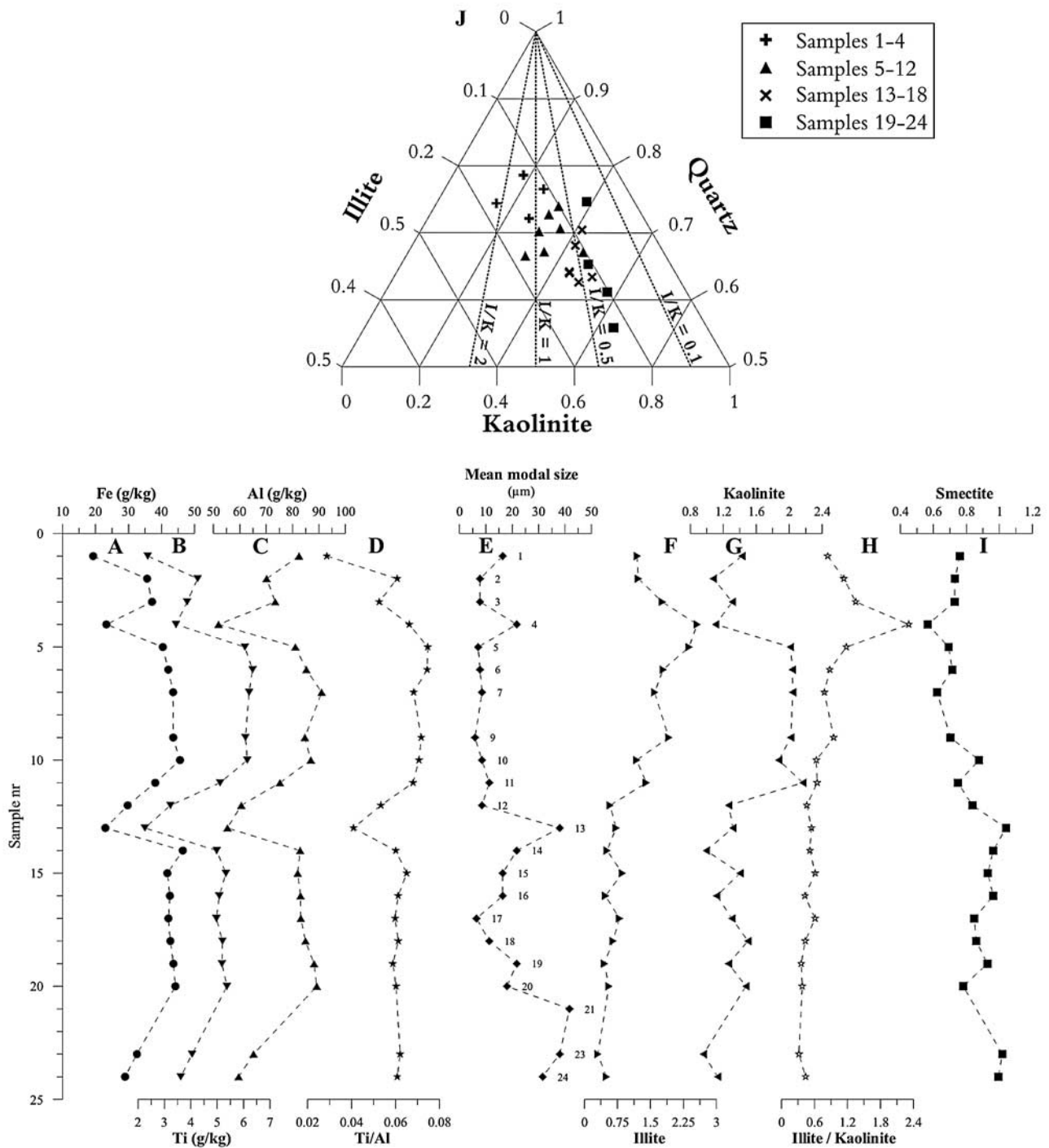


**Figure 5.** Bulk chemical, physical, and clay mineralogical characteristics of all dust samples. (a) Iron content (g/kg, circles), (b) titanium content (g/kg, inverted triangles), (c) aluminium content (g/kg, triangles), (d) titanium-aluminium ratio (solid stars), (e) mean modal size ( $\mu\text{m}$ , diamonds), (f) illite content (normalized to total counts, right-pointing triangles), (g) kaolinite content (normalized to total counts, left-pointing triangles), (h) illite/kaolinite ratio (open stars), (i) smectite content (normalized to total counts, squares), and (j) quartz-illite-kaolinite ternary diagram, with the samples plotted in the same groups as in Figure 3.

of the quartz-illite-kaolinite content [cf. *Caquineau et al.*, 2002; *Chiapello et al.*, 1997] does show a generally north-south trend (Figure 5j). Smectite, a mineral that is indicative for wet tropical soils [e.g., *Biscaye*, 1965], seems to be the only mineral that shows a slight increase toward the south.

#### 4.4. Meteorology

[22] To get an impression of the vertical structure of the atmosphere, weather balloons were launched twice daily by the “Deutsche Wetterdienst” [see *Schulz et al.*, 1998] during the cruise in 1998. Figure 6 shows some examples

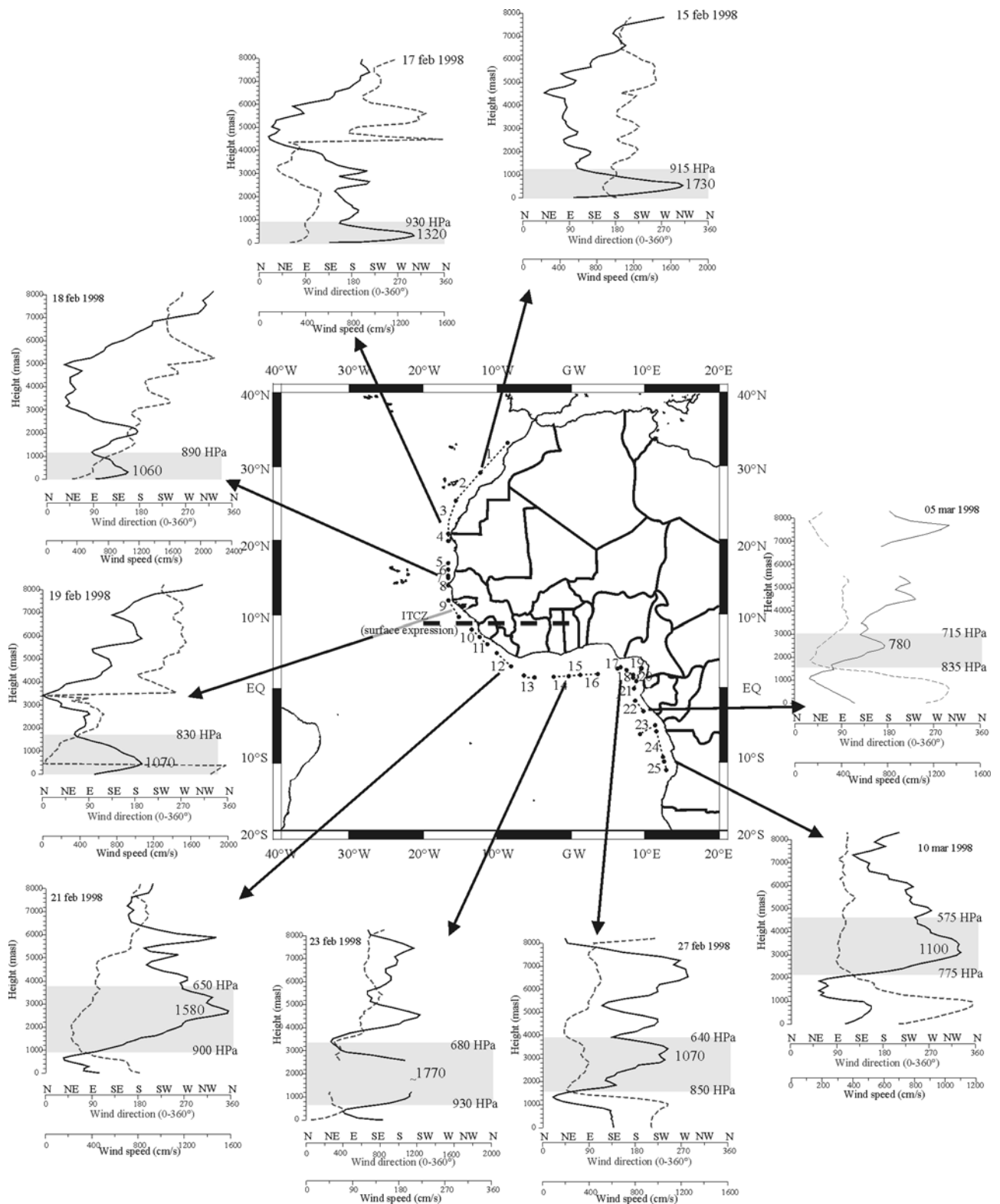


**Figure 6.** Meteorological data for different days during the sample interval, as measured by weather balloons from the Deutsche Wetterdienst onboard FS *Meteor* during cruise M41/1. Dashed curves indicate wind direction (0°–360°). Solid curves indicate wind strength (cm/s). Grey shading indicates layer of maximum sediment transporting capacity. Note that this layer shifts up in the atmosphere going from north to south. See also Table 1.



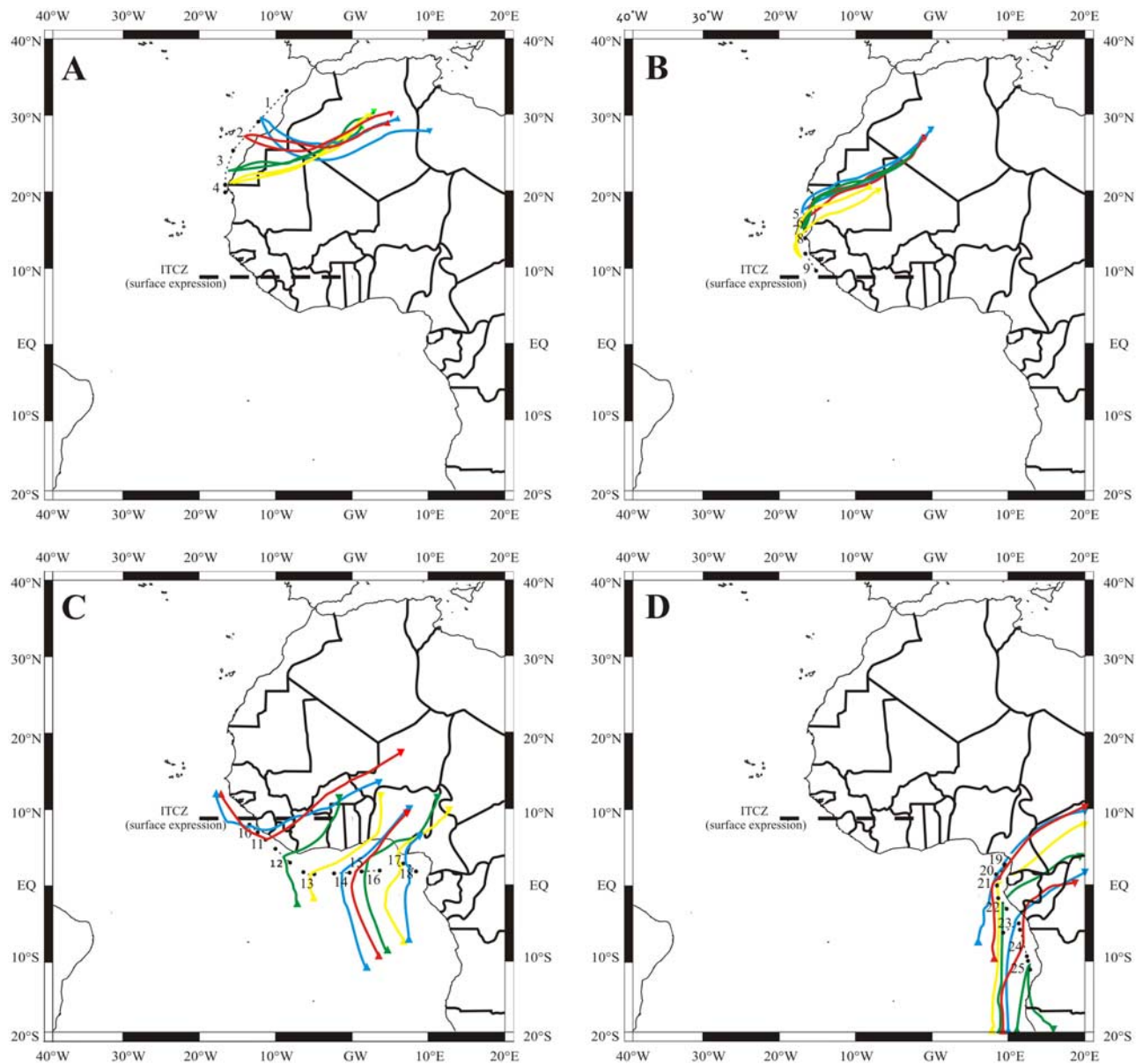


**Figure 7.** Grouped HY-SPLIT 4 (HY-SPLIT model access available from NOAA Air Resources Laboratory Real-time Environmental Applications and Display System at <http://www.arl.noaa.gov/ready/hysplit4.html>) 4-day back trajectories for four different sample intervals. (a) Samples 1–4, (b) samples 5–9, (c) samples 10–18, and (d) samples 19–25.

of vertical profiles of wind speed and direction through the atmosphere at several sampling points along the cruise track. The lowest layer of maximum wind speeds, indicated by grey shading, is about at sea level in the northern part of the profile; the northeast trades. These northeastern winds are raised to higher altitudes ( $>1000$  m) in the southern part (21 February and later).

#### 4.5. Back Trajectories

[23] On the basis of the meteorological observations we determined for each individual sample the atmospheric levels for which transporting capacities were highest. Using the HY-SPLIT 4 model of NOAA (HY-SPLIT model access available from NOAA Air Resources Laboratory READY at

<http://www.arl.noaa.gov/ready/hysplit4.html>), 4-day back trajectories for these particular levels were calculated for all samples (Figure 7), as well as conditions at 10 m asl (the altitude of the dust samplers on the ship). From these calculations it appears that sample 1 stands out with back trajectories leading as far back as Libya, but samples 2–9 (Figures 7a and 7b) all point to an Algerian source of sediments. From sample 10 on, there is a clear difference between surface winds (triangle) and higher-level winds (inverted triangle), due to crossing the surface expression of the ITCZ. The low-level winds all point to an oceanward origin, clearly unable to carry any aerosol dust. In contrast, the higher-level 4-day back trajectories for samples 10–18 (Figure 7c) actually all suggest that the source of wind-

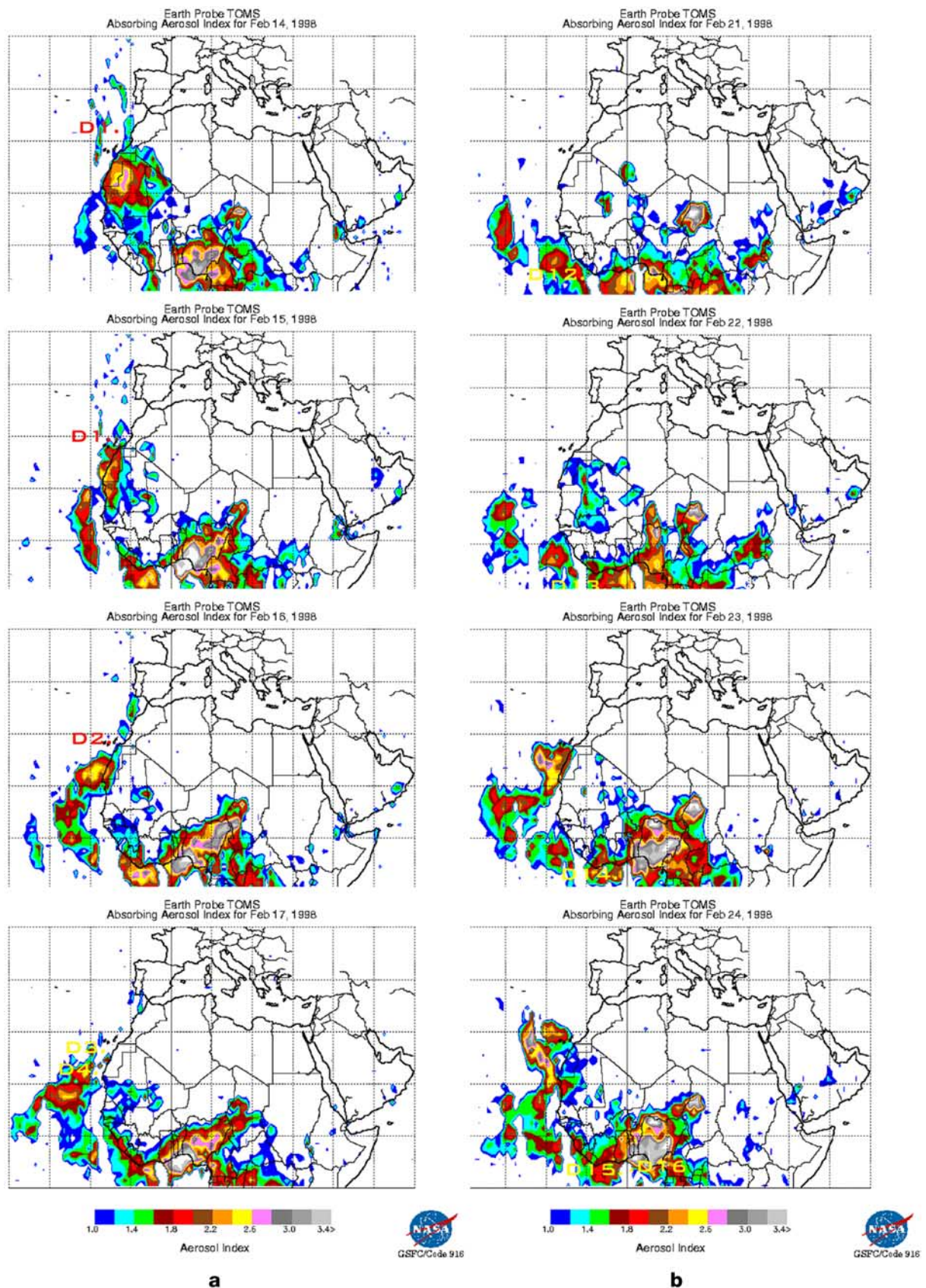


**Figure 8.** Daily TOMS (<http://jwocky.gsfc.nasa.gov>) data for two time intervals. Locations of the aerosol samples at the time of dust collection are indicated in the individual TOMS images ( $D_{xx}$ ): (a) 14–17 February 1998, samples 1–4, and (b) 21–24 February 1998, samples 12–16. Images courtesy of Laboratory for Atmospheres, Goddard Space Flight Center.

blown dusts lies in the central Sahara/Chad, an observation that has been made already more than 200 years ago [Dobson, 1781]. This clearly illustrates that the ITCZ is not a boundary to dust deposition in the equatorial eastern Atlantic. The trajectories for samples 19–24 collected offshore Cameroon, equatorial Guinea, and Gabon (Figures 1 and 7d) point to a source area located southeast of Chad, in central Africa. For the last sample (25, Figure 7d) both the low-level and high-level winds point to a Namibian source of the dust-carrying winds.

#### 4.6. Satellite Imagery

[24] The daily TOMS images clearly show that dust is generated in a few localities, from which the dust is successively transported through the atmosphere. Two sets of images are shown here, illustrating the development of dust outbreaks in Mauritania and Niger (Figure 8a) and Chad (Figure 8b), respectively.

### 5. Discussion

[25] The grain-size distributions of the aerosol samples illustrate the large spread in the size of eolian dust that can be found in the deep sea. However, it also shows that the assumption that all sediments coarser than a certain cutoff value (e.g.,  $>6 \mu\text{m}$  [cf. Sarnthein *et al.*, 1981]) are of wind-blown origin is too simple. Although the aerosol samples compare well with sediment trap and surface sediments from the same regions (Figure 4), some care has to be taken because these were obtained using different methods [Ratmeyer *et al.*, 1999]. Besides, there may be differences between the grain-size distributions of aerosol samples, terrigenous fraction of sediments in traps and on the sediment surface due to, e.g., advection of river-derived sediments, current winnowing of sediments during settling through the water column, and alteration of the particles after deposition. Nevertheless, especially the sediments off Cape Blanc compare very well with each other, probably because this is one of the regions where massive dust outbreaks occur throughout the winter season [Torres-Padrón *et al.*, 2002].

[26] Differences between the grain-size distributions collected near Cape Verde are predominantly ascribed to variations in wind strength and dust availability; both the trap sample (collected in 1993, few weeks) and the aerosol sample (collected in February 1998, few hours) are relative “snap shots” compared to the much larger time span over which sediments are deposited on the seafloor (sedimentation rates are a few mm/yr), and hence they are highly susceptible to changes in wind strength and dust season. This may also explain why the surface sediments off Cape Verde are coarser grained than the aerosol samples, beside the possibility of currents winnowing the fine fraction of the settling aerosols through the water column.

[27] No trap samples were available for the Canary Islands site, but the sediment surface sample (Figure 4b) is again coarser grained than the aerosol sample. This is ascribed to the above mentioned current winnowing and variations in wind strength. The characteristic SAL that occurs in the summer season was obviously not represented in our aerosol samples. However, due to the high altitudes at which this SAL takes place, we may assume that the size of

the dust that is transported with the SAL is much finer grained. However, we observe that the sediments from the seafloor [Ratmeyer *et al.*, 1999] are coarser grained relative to our aerosols. Therefore we hypothesize that the major part of wind-blown dusts deposited off northwest Africa are transported by the trades, and not by the SAL, which carries relatively fine-grained dust further offshore.

[28] This study also shows that great care has to be taken with the interpretation of 4-day back trajectories. They can be used as a coarse estimate of where the air masses originated from but do not necessarily lead back to the source area of the dust. The first coarse estimate of the source of wind-blown sediments was published by Dobson [1781], who applied a triangulation technique based on three wind direction measurements at three different locations along the northwest African coast. Thus he placed the source area of the Harmattan in the Darfur area of western Sudan [McTainsh, 1982], not too far off from where it is generally accepted to come from: the Bodélé depression in Chad. Back trajectories of air parcels have been frequently used to determine the source of aerosols [Caquineau *et al.*, 2002; Chiapello *et al.*, 1997; Guieu *et al.*, 2002; Schefuß *et al.*, 2003]. One shortcoming of this method is that 4 days may not be long enough to trace the air parcels back to where the actual dust was entrained. As shown in Figure 7, some trajectories seem to point to known dust source areas but do not reach them in 4 days (e.g., Figure 7c, no trajectories make it back to the Bodélé depression). However, we have shown that selective transport of eolian dust strongly depends on path length as well as altitude of the transported dust, like, e.g., the general fining trend due to higher altitudes of the transporting wind layer. Therefore we chose to restrict the back trajectory calculations to 4 days, since even during these 4 days there may be selective transport processes. Another feature that has to be taken into account is the location of entrainment of the aerosols. This can be illustrated by the fact that samples 1–4 are quite different both in grain-size distributions as well as in chemical and mineralogical composition. Apparently, this can be explained by the 4-day back trajectories (Figure 7a), which show that there is a relatively large spread in source areas and paths of the trajectories. However, when considering the TOMS images, it can be seen that there has been a dust outbreak from Mauritania (Figure 8a), just shortly before sample 4 was collected offshore. This clearly illustrates that back trajectories do not necessarily lead back to the ultimate source region of the dust, but additional information is required. The trajectory itself may show what the path has been of the parcel of air of interest, but one can never reconstruct where the aerosols have been picked up by this parcel of air.

[29] Furthermore, we have shown that completely different sources and transport pathways may produce very similar grain-size distributions. For example, samples 5–10 and 12 show very similar grain-size distributions (Figure 3), but the back trajectories of samples 10–12 clearly trace back to a different source region (Figures 7b and 7c). This observation is further supported by the chemical composition of these samples (Figures 5a–5d). However, the Ti/Al ratio, which is commonly used as a proxy for grain size in deep-marine sediments, decreases from sample 10 to 12, suggesting a decrease in the size distribution of samples

10–12, which is not observed. The chemical composition of the aerosols can be similarly misleading with respect to their provenance. Sample 10, for example, has a chemical composition that is very similar to the ones of the samples collected further north (Figures 5a–5d).

[30] Another characteristic that is very similar for samples 5–9 is their kaolinite content (Figure 5g). Again, sample 10 would at first sight also classify to belong to this group, although the illite content does not show such a clear pattern.

[31] Samples 10–24 were all collected south of the surface expression of the ITCZ. However, as was mentioned before, the vertical structure of the ITCZ is not a perpendicular one but slightly tilted toward the north [e.g., Hamilton and Archbold, 1945]. Hence it can be expected that the relatively sharp boundary formed by the ITCZ will not be reflected as prominent in the distribution of aerosols collected at sea level, since aerosols may also settle from higher levels in the atmosphere. The 4-day back trajectories clearly show the complicated structure of the atmosphere in the vicinity of the ITCZ; although the very weak surface winds are from the south to southeast, material is transported from the northeast at higher altitudes due to the tilted vertical structure of the ITCZ. This explains the relatively high dust load and relatively coarse-grained sediments south of the surface expression of the ITCZ (samples 13–18). The gradual decrease of the grain-size distributions from sample 13 to 18 may be explained by the increasing altitudes to which the northeast trades are “pushed” by the ITCZ. During the ascent into the atmosphere the winds obviously lose their transporting capacity. This observation is confirmed by aerosols collected on Gran Canaria, one of the Canary Islands [Torres-Padrón *et al.*, 2002], at an altitude of ~2000 m, which are predominantly clay/very fine silt sized (0.6–5  $\mu\text{m}$ ). This stresses the importance of the trade winds as the main carrier of silt-sized aerosols and moderates the role of the SAL for the deposition of proximal dust.

[32] The similar chemical compositions of samples 14–20 is partly confirmed by the 4-day back trajectories, which all indicate a central African source of dust. However, the TOMS images indicate the importance of the Bodélé depression in Chad as a source of aerosols, and all trajectories pass through the dust outbreaks from this area (Figure 8b), stressing the capability of central African dust to cross the ITCZ.

[33] The meteorological observations south of the equator show very low wind speeds from westerly directions at sea surface and an easterly direction only at high altitudes (1600–2000 m). Despite these weak surface winds that blow from the central Atlantic Ocean, we still observe relatively coarse grain-size distributions (samples 19–23), and therefore we think that the southeast trades carry this dust to the Atlantic Ocean. This conclusion is supported by carbon isotopes of plant waxes [Schefuß *et al.*, 2003] and bulk carbon and nitrogen isotopes (G. Lavik, unpublished results, 2000) that indicate that these samples originate from tropical Africa.

[34] The mineralogical content of the samples does not show as clear patterns as the grain-size distributions and bulk chemistry. This could be explained by the fact that the bulk samples were considered, instead of the clay (<2  $\mu\text{m}$ ) fraction, besides general difficulties in preparing the very

small amounts of samples. However, the comparison of the quartz-illite-kaolinite content [cf. Caquineau *et al.*, 2002; Chiapello *et al.*, 1997] does show a generally north-south trend (Figure 5j). The only mineral that shows a southward increase in occurrence is smectite, a mineral that is indicative for wet tropical soils [e.g., Biscaye, 1965].

[35] This study shows the advantage of combining meteorological (local, from weather balloons as well as regional, from back trajectory calculations) and satellite data to interpret variations in sedimentological and bulk chemical and mineralogical characteristics of aerosols. We have shown that the altitude of the air layers of maximum transporting capacities varies strongly, indicating that the often applied [e.g., Romero *et al.*, 2003; Viana *et al.*, 2002] boundaries of 850 hPa ( $\approx$ 1500 m asl) and 500 hPa ( $\approx$ 6000 m asl) do not necessarily represent the layers along which dust is transported.

## 6. Conclusions

[36] The study of present-day dust samples is indispensable for the characterization of eolian dust deposited in deep sea sediments. The combined sedimentological, bulk chemical, and mineralogical characteristics of the actual aerosols can be used to characterize source areas of wind-blown dusts, but meteorological and atmospheric data are essential for detailed provenance studies. The combination of meteorological data and satellite data provides a powerful tool to trace back aerosols to their source areas. Furthermore, we have shown that selective transport processes lead to a major size decrease of aerosols on their way up in the atmosphere, decreasing the importance of the SAL as a major transporting agent of proximal dust. Furthermore, we have shown that backward air parcel trajectories do not necessarily lead back to the source of dust as the winds may pick up dust from local outbreaks along their pathways to the site of deposition.

[37] **Acknowledgments.** We thank the captain, crew, and scientists aboard FS *Meteor* (M41/1) for their help with the aerosols collection. We are indebted to Christoph Joppich and Wolf-Thilo Ochsenschirt from the Deutsche Wetterdienst for their atmospheric measurements. Sjerry van de Gaast (Royal Netherlands Institute for Sea Research (NIOZ)) is thanked for help with X-ray diffraction, Wim Boer (NIOZ) is thanked for help with grain-size analysis. This manuscript greatly benefited from the reviews by Grant McTainsh and an anonymous reviewer. Financial support was provided by the Deutsche Forschungsgemeinschaft as part of the DFG-Research Center “Ocean Margins” of the University of Bremen. This is publication RCOM0208.

## References

- Arimoto, R., B. J. Ray, N. F. Lewis, U. Tomza, and R. A. Duce (1997), Mass-particle size distributions of atmospheric dust and the dry deposition of dust to the remote ocean, *J. Geophys. Res.*, *102*(D13), 15,867–15,874.
- Biscaye, P. (1965), Mineralogy and sedimentation of recent deep-sea clay in the Atlantic Ocean and adjacent seas and oceans, *Geol. Soc. Am. Bull.*, *76*, 803–832.
- Caquineau, S., A. Gaudichet, L. Gomes, M.-C. Magonthier, and B. Chatenet (1998), Saharan dust: Clay ratio as a relevant tracer to assess the origin of soil-derived aerosols, *Geophys. Res. Lett.*, *25*(7), 983–986.
- Caquineau, S., A. Gaudichet, L. Gomes, and M. Legrand (2002), Mineralogy of Saharan dust transported over northwestern tropical Atlantic Ocean in relation to source regions, *J. Geophys. Res.*, *107*(D15), 4251, doi:10.1029/2000JD000247.
- Carlson, T. N., and J. M. Prospero (1972), The large-scale movement of Saharan air outbreaks over the northern equatorial Atlantic, *J. Appl. Meteorol.*, *11*(2), 283–297.

- Chester, R., and L. R. Johnson (1971), Atmospheric dusts collected off the West African coast, *Nature*, **229**, 105–107.
- Chiapello, I., G. Bergametti, B. Chatenet, P. Bousquet, F. Dulac, and S. Soares (1997), Origins of African dust transported over the north-eastern tropical Atlantic, *J. Geophys. Res.*, **102**(D12), 13,701–13,709.
- Chiapello, I., J. M. Prospero, J. R. Herman, and N. C. Hsu (1999), Detection of mineral dust over the North Atlantic Ocean and Africa with the Nimbus 7 TOMS, *J. Geophys. Res.*, **104**(D8), 9277–9291.
- d'Almeida, G. A. (1989), Desert aerosol: Characteristics and effects on climate, in *Palaeoclimatology and Palaeometeorology: Modern and Past Patterns of Global Atmospheric Transport*, edited by M. Leinen and M. Sarnthein, pp. 311–338, Springer, New York.
- Darwin, C. (1846), An account of the fine dust which often falls on vessels in the Atlantic Ocean, *Q. J. Geol. Soc. London*, **2**, 26–30.
- deMenocal, P. B., J. Ortiz, T. P. Guilderson, J. Adkins, M. Sarnthein, L. Baker, and M. Yarusinsky (2000), Abrupt onset and termination of the African Humid Period: Rapid climate responses to gradual insolation forcing, *Quat. Sci. Rev.*, **19**, 347–361.
- Dobson, M. (1781), An account of the Harmattan, a singular African wind, *Philos. Trans. R. Soc. London*, **71**, 46–57.
- Duce, R. A., P. S. Liss, J. T. Merrill, E. L. Atlas, and P. Buat-Ménard (1991), The atmospheric input of trace species to the world ocean, *Global Biogeochem. Cycles*, **5**(3), 193–259.
- Glaccum, R. A., and J. M. Prospero (1980), Saharan aerosols over the tropical North Atlantic—Mineralogy, *Mar. Geol.*, **37**(3–4), 295–321.
- Guieu, C., M.-D. Loÿe-Pilot, C. Ridame, and C. Thomas (2002), Chemical characterization of the Saharan dust end-member: Some biogeochemical implications for the western Mediterranean Sea, *J. Geophys. Res.*, **107**(D15), 4258, doi:10.1029/2001JD000582.
- Hamilton, R. A., and J. W. Archbold (1945), Meteorology of Nigeria and adjacent territory, *Q. J. Geol. Soc. London*, **71**, 231–265.
- Hastenrath, S. (1985), *Climate and Circulation of the Tropics*, 455 pp., Springer, New York.
- Herman, J. R., P. K. Bhartia, O. Torres, C. Hsu, C. Seftor, and E. Celarier (1997), Global distribution of UV-absorbing aerosols from Nimbus 7/TOMS data, *J. Geophys. Res.*, **102**(D14), 16,911–16,922.
- Holz, C., J.-B. W. Stuut, and R. Henrich (2004), Terrigenous sedimentation processes along the continental margin off NW-Africa: Implications from grain-size analyses of surface sediments, *Sedimentology*, **51**(5), 1145–1154.
- Husar, R. B., J. M. Prospero, and L. L. Stowe (1997), Characterization of tropospheric aerosols over the oceans with the NOAA advanced very high resolution radiometer optical thickness operational product, *J. Geophys. Res.*, **102**(D14), 16,889–16,909.
- Kalu, A. E. (1979), The African dust plume: Its characteristics and propagation across West Africa in winter, *SCOPE*, **14**, 95–118.
- Kiefert, L. (1994), Characteristics of wind transported dust in eastern Australia, Ph.D. thesis, Griffith Univ., Brisbane, Australia.
- Kiefert, L., G. H. McTainsh, and W. G. Nickling (1996), Sedimentological characteristics of Saharan and Australian dusts, in *The Impact of Desert Dust Across the Mediterranean*, edited by S. Guerzoni and R. Chester, pp. 183–190, Springer, New York.
- Kohfeld, K. E., and S. P. Harrison (2001), DIRTMAP: The geological record of dust, *Earth Sci. Rev.*, **54**(1), 81–114.
- Konert, M., and J. Vandenberghe (1997), Comparison of laser grain size analysis with pipette and sieve analysis: A solution for the underestimation of the clay fraction, *Sedimentology*, **44**(3), 523–535.
- Koopmann, B. (1981), Sedimentation von Saharastaub im subtropischen Nordatlantik während der letzten 25.000 Jahre, *Meteor. Forschungsber., Reihe C*, **35**, 23–59.
- Krumbein, W. C., and F. J. Pettijohn (1938), *Manual of Sedimentary Petrography*, 549 pp., Appleton-Century-Crofts, New York.
- Martin, J. H., and S. E. Fitzwater (1988), Iron deficiency limits phytoplankton growth in the northeast Pacific subarctic, *Nature*, **331**, 341–343.
- McTainsh, G. H. (1980), Harmattan dust deposition in northern Nigeria, *Nature*, **286**, 587–588.
- McTainsh, G. H. (1982), Harmattan dust, aeolian mantles and dunesands of central northern Nigeria, Ph.D. thesis, Macquarie Univ., Sydney, Australia.
- McTainsh, G. H., and P. H. Walker (1982), Nature and distribution of Harmattan dust, *Z. Geomorphol.*, **26**(4), 417–435.
- Middleton, N. J., and A. S. Goudie (2001), Saharan dust: Sources and trajectories, *Trans. Inst. Br. Geogr.*, **26**(2), 165–181.
- Moreno, A., J. Targarona, J. Henderiks, M. Canals, T. Freudenthal, and H. Meggers (2001), Orbital forcing of dust supply to the North Canary Basin over the last 250 kyr, *Quat. Sci. Rev.*, **20**, 1327–1339.
- Muhs, D. R., C. A. Bush, K. C. Stewart, T. R. Rowland, and R. C. Crittenden (1990), Geochemical evidence of Saharan dust parent material for soils developed on Quaternary limestones of Caribbean and western Atlantic islands, *Quat. Res.*, **33**, 157–177.
- Nicholson, S. E. (2000), The nature of rainfall variability over Africa on time scales of decades to millennia, *Global Planet. Change*, **26**, 137–158.
- Oliver, J. E., and R. W. Fairbridge (1987), *The Encyclopedia of Climatology*, pp. 986, Van Nostrand Reinhold, Hoboken, N. J.
- Ott, S.-T., A. Ott, D. W. Martin, and J. A. Young (1991), Analysis of a trans-Atlantic Saharan dust outbreak based on satellite and GATE data, *Mon. Weather Rev.*, **119**(8), 1832–1850.
- Pérez-Marrero, J., O. Llinás, L. Maroto, M. J. Rueda, and A. Cianca (2002), Saharan dust storms over the Canary Islands during winter 1998 as depicted from the advanced very high-resolution radiometer, *Deep Sea Res., Part II*, **49**(17), 3465–3479.
- Prospero, J. M. (1990), Mineral-aerosol transport to the north Atlantic and north Pacific: The impact of African and Asian sources, in *The Long-Range Atmospheric Transport of Natural and Contaminant Substances*, edited by A. H. Knap, pp. 59–86, Springer, New York.
- Prospero, J. M. (1996), The atmospheric transport of particles to the ocean, in *Particle Flux in the Ocean*, edited by V. Ittekkot et al., pp. 19–52, John Wiley, Hoboken, N. J.
- Prospero, J. M., and P. J. Lamb (2003), African droughts and dust transport to the Caribbean: Climate change implications, *Science*, **302**, 1024–1027.
- Prospero, J. M., R. A. Glaccum, and R. T. Nees (1981), Atmospheric transport of soil dust from Africa to South America, *Nature*, **289**, 570–572.
- Prospero, J. M., P. Ginoux, O. Torres, S. E. Nicholson, and T. E. Gill (2002), Environmental characterization of global sources of atmospheric soil dust identified with the NIMBUS 7 Total Ozone Mapping Spectrometer (TOMS) absorbing aerosol product, *Rev. Geophys.*, **40**(1), 1002, doi:10.1029/2000RG000095.
- Pye, K. (1987), *Aeolian Dust and Dust Deposits*, 334 pp., Elsevier, New York.
- Ratmeyer, V., G. Fischer, and G. Wefer (1999), Lithogenic particle fluxes and grain size distributions in the deep ocean off northwest Africa: Implications for seasonal changes of aeolian dust input and downward transport, *Deep Sea Res., Part I*, **46**(8), 1289–1337.
- Rea, D. K. (1994), The paleoclimatic record provided by eolian deposition in the deep sea: The geologic history of wind, *Rev. Geophys.*, **32**(2), 159–195.
- Reed, R. J., D. C. Norquist, and E. E. Recker (1977), The structure and properties of African wave disturbances as observed during phase III of GATE, *Mon. Weather Rev.*, **105**(3), 317–373.
- Rognon, P., and G. Coudé-Gaussen (1996), Paleoclimates off NW Africa (28–35°N) about 18,000 yr BP based on continental eolian deposits, *Quat. Res.*, **46**, 118–126.
- Romero, O. E., L. Dupont, U. Wyputta, S. Jahns, and G. Wefer (2003), Temporal variability of fluxes of eolian-transported freshwater diatoms, phytoliths, and pollen grains off Cape Blanc as reflection of land-atmosphere-ocean interactions in northwest Africa, *J. Geophys. Res.*, **108**(C5), 3153, doi:10.1029/2000JC000375.
- Ruddiman, W. F. (2001), *Earth's Climate—Past and Future*, 465 pp., W. H. Freeman, New York.
- Sarnthein, M., G. Tetzlaff, B. Koopmann, K. Wolter, and U. Pflaumann (1981), Glacial and interglacial wind regimes over the eastern subtropical Atlantic and north-west Africa, *Nature*, **293**, 193–196.
- Sarnthein, M., J. Thiede, U. Pflaumann, H. Erlenkeuser, D. Fütterer, B. Koopmann, H. Lange, and E. Seibold (1982), Atmospheric and oceanic circulation patterns off northwest Africa during the past 25 million years, in *Geology of the Northwest African Continental Margin*, edited by U. Von Rad, K. Hinz, M. Sarnthein, and E. Seibold, pp. 545–604, Springer, New York.
- Schefuß, E., V. Ratmeyer, J.-B. W. Stuut, J. H. F. Jansen, and J. S. Sinninghe Damsté (2003), Carbon isotope analyses of n-alkanes in dust from the lower atmosphere over the central eastern Atlantic, *Geochim. Cosmochim. Acta*, **67**(10), 1757–1767.
- Schulz, H. D., et al. (1998), Report and preliminary results of Meteor Cruise M41/1, in *Berichte aus dem Fachbereich Geowissenschaften der Universität Bremen*, **114**, 124 pp., Univ. at Bremen, Bremen, Germany.
- Schütz, L., R. Jaenicke, and H. Pietrek (1981), Saharan dust transport over the North Atlantic Ocean, *Spec. Pap. Geol. Soc. Am.*, **186**, 87–100.
- Shinn, E. A., G. W. Smith, J. M. Prospero, P. Betzer, M. L. Hayes, V. Garrison, and R. T. Barber (2000), African dust and the demise of Caribbean coral reefs, *Geophys. Res. Lett.*, **27**(19), 3029–3032.
- Simoneit, B. R. T., R. E. Cox, and L. J. Standley (1988), Organic matter of the troposphere—IV. Lipids in Harmattan aerosols of Nigeria, *Atmos. Environ.*, **22**(5), 983–1004.
- Stuut, J.-B. W. (2001), Late Quaternary southwestern African terrestrial-climate signals in the marine record of Walvis Ridge, SE Atlantic Ocean, Ph.D. thesis, 128 pp., Utrecht Univ., Utrecht, Netherlands.

- Swap, R., S. Ulanski, M. Cobbett, and M. Garstrang (1996), Temporal and spatial characteristics of Saharan dust outbreaks, *J. Geophys. Res.*, *101*(D2), 4205–4220.
- Talbot, R. W., R. C. Harriss, E. V. Browell, G. L. Gregory, D. I. Sebacher, and S. M. Beck (1986), Distribution and geochemistry of aerosols in the tropical North Atlantic troposphere: Relationship to Saharan dust, *J. Geophys. Res.*, *91*(D4), 5173–5182.
- Torres-Padrón, M. E., M. D. Gelado-Caballero, C. Collado-Sánchez, V. F. Siruela-Matos, P. J. Cardona-Castellano, and J. J. Hernández-Brito (2002), Variability of dust inputs to the CANIGO zone, *Deep Sea Res., Part II*, *49*(17), 3455–3464.
- Van der Gaast, S. (1991), Mineralogical analysis of marine particles by X-ray powder diffraction, in *Marine Particles: Analysis and Characterization*, *Geophys. Monogr. Ser.*, vol. 63, edited by D. C. Hurd and D. W. Spencer, pp. 343–362, AGU, Washington, D. C.
- Viana, M., X. Querol, A. Alastuey, E. Cuevas, and S. Rodríguez (2002), Influence of African dust on the levels of atmospheric particulates in the Canary Islands air quality network, *Atmos. Environ.*, *36*(38), 5861–5875.
- Wilke, B.-M., B. J. Duke, and W. L. O. Jimoh (1984), Mineralogy and chemistry of Harmattan dust in Northern Nigeria, *Catena*, *11*(1), 91–96.
- Wilson, I. G. (1971), Desert sandflow basins and a model for the development of ergs, *Geogr. J.*, *137*, 180–198.
- Zabel, M., T. Bickert, L. Dittert, and R. R. Häse (1999), Significance of the sedimentary Al:Ti ratio as an indicator for variations in the circulation patterns of the equatorial North Atlantic, *Paleoceanography*, *14*(6), 789–799.
- Zabel, M., R. R. Schneider, T. Wagner, A. T. Adegbe, U. De Vries, and S. Kolonic (2001), Late Quaternary climate changes in central Africa as inferred from terrigenous input to the Niger Fan, *Quat. Res.*, *56*, 207–217.

---

P. Helmke, V. Ratmeyer, E. Schefuß, J.-B. Stuut, and M. Zabel, Research Center Ocean Margins, Universität Bremen, Klagenfurterstrasse 2, Bremen, D-28334, Germany. (jbstuut@rcom-bremen.de)

G. Lavik, Max Planck Institute for Marine Microbiology, Celciusstrasse 1, Bremen, D-28359, Germany.

R. Schneider, Département Géologie et Océanographie, UMR-CNRS 5805 EPOC, Université Bordeaux I, Avenue des Facultés, F-33405 Talence, France.